Journal of Engineering Physics and Thermophysics, Vol. 83, No. 2, 2010

ANALYSIS OF THE EFFECTS OF INLET TEMPERATURE FREQUENCY IN FULLY DEVELOPED LAMINAR DUCT FLOWS

A. Hadiouche and K. Mansouri

UDC 536.2

Unsteady heat transfer for a fully developed laminar flow inside a parallel-plate channel and circular duct that are subjected to a periodically varying inlet temperature is studied. The thermal capacitance of the duct wall and the boundary condition that accounts for external convection are considered. An exact solution is presented for this extended Graetz problem as the result of using a new methodology based on a variational method. The quasi-steady approach that employs a heat transfer coefficient at the liquid–solid interface is also investigated, and the results are compared with the variational solution. The damping and phase lag coefficients as functions of the inlet temperature frequency are presented in graphical form.

Keywords: *conjugated forced convection, internal laminar flow, periodic inlet temperature, quasi-steady model, analytical solution.*

Introduction. Knowledge of the thermal response of unsteady laminar and turbulent flows inside ducts with periodically varying inlet temperature is important for many engineering applications where hot and cold fluids pass in succession, such as in regenerative and recuperative heat exchangers. Investigations of periodic laminar forced convection and turbulent duct flows have been performed by numerous researchers [1–17]. In works [1–6], only the fluid energy equation was solved without conjugation with the walls. Kakaç and Yener [1, 2] considered a transient energy equation with the inlet temperature varying with time for slug flow and turbulent heat transfer between two parallel plates. Cotta and Ozisik [3] studied laminar forced convection with periodic variations of inlet temperature without conjugation with the walls for both parallel plates and circular ducts. In [7–13], the methodologies used in the previous works were advanced further by considering the effects of the heat capacity of the duct wall. Sparrow and Farias [7] appear to be the first to include the effect of wall conjugation. They investigated the slug flow periodic laminar forced convection in a parallel-plate channel, where the wall temperature was dynamically determined by a balance of the heat transfer rate and energy storage. Cotta et al. [8] utilized the solution methodology suggested in [7] to consider the conjugated laminar forced convection in parallel-plate ducts and circular tubes for a slug flow with periodically varying inlet temperature. The sign-count modifying method was adopted for determination of complex eigenvalues. Kim and Ozisik [9] treated the same problem with a parabolic velocity profile; the resulting complex eigenvalue problem was solved by using the Runge–Kutta method. Travelho and Santos [10, 11] solved the same problem as that considered in [7, 8] with the same physical conditions by applying the Laplace transform. The original solution was obtained numerically for plane and cylindrical configurations. Kakaç and Li [12, 13] used the theoretical analysis of [1] to involve the effects of wall thermal capacitance and external convection. In [7–13], the wall effects are included in the thermal boundary condition at the fluid–wall interface.

The same problem that takes into account heat axial diffusion and transversal heat conduction in a duct wall was investigated by several authors [14–18]. There exist other studies on the extensions of the Graetz problem. Among important extensions are the consideration of slip flow [19, 20], non-Newtonian fluids [21, 22], and viscous dissipation [23].

In a practical case, the thermal design engineer is responsible for determining the thermal response of heat exchangers. The simplest approach consists in using a standard quasi-steady model with a constant heat transfer coefficient at the interface. In all the studies noted [1–22], the effects of the inlet temperature frequency on the heat transfer coefficient remain untreated. To our mind, Sparrow and Farias [7] are the only researchers who compared the quasi-steady approach (QSA) result and the complete solution for a laminar slug flow in a par-

University M. Bougara of Boumerdes, Faculty of Engineering Science, Department of Energy, Boumerdes 35000, Algeria; email: manskac@yahoo.fr. Published in Inzhenerno-Fizicheskii Zhurnal, Vol. 82, No. 2, pp. 357–368, March–April, 2010. Original article submitted October 10, 2008.

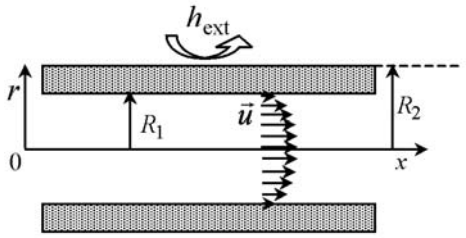

Fig. 1. Geometry of the problem.

allel-plate channel. That is why in this work the accuracy and limitation of the QSA for a laminar forced convection inside a parallel-plate channel and a circular duct with a periodically varying inlet temperature are investigated. A new methodology is obtained for this extended Graetz problem by using the variational Ritz technique. The effects of the dimensionless frequency of the inlet temperature oscillations on the damping and phase lag coefficients are illustrated. The results given by this exact solution are compared with those obtained by the QSA.

Variational Model. We consider unsteady forced convection with a fully developed laminar flow inside the thermal entrance region of a channel (circular or parallel-plate) subjected to a periodic variation of the inlet temperature as shown in Fig. 1. The mathematical formulation of this transient conjugated problem is given by

$$\frac{\partial T}{\partial t} + u(r)\frac{\partial T}{\partial x} = \alpha_{\rm f}\frac{1}{r^m}\frac{\partial}{\partial r}\left(r^m\frac{\partial T}{\partial r}\right), \quad 0 < r < R_1, \quad x > 0, \quad t > 0; \tag{1}$$

$$T = T_\infty + T_0 \sin \delta t \quad \text{at} \quad x = 0, \quad 0 \le r \le R_1, \quad t > 0; \tag{1a}$$

$$\frac{\partial T}{\partial r} = 0 \quad \text{at} \quad r = 0, \quad x > 0, \quad t > 0; \tag{1b}$$

$$(\rho C)_{\rm s}(R_2 - R_1)\frac{\partial T_{\rm w}}{\partial t} + h_{\rm ext}(T_{\rm w} - T_\infty) + k_{\rm f}\frac{\partial T}{\partial r} = 0 \quad \text{at} \quad r = R_1, \quad x > 0, \quad t > 0, \tag{1c}$$

where $m = 0$ for a parallel-plate channel and $m = 1$ for a circular duct. Equation (1c) represents the third kind boundary condition that accounts for both the external convection and wall heat capacitance effects. At the wall–fluid interface, the connection is established by using the continuity of temperatures:

$$T(x, r, t) = T_{\rm w}(x, t) \quad \text{at} \quad r = R_1, \quad x > 0, \quad t > 0. \tag{1d}$$

The problem expressed in the dimensionless form is

$$\frac{\partial T^+}{\partial t^+} + u^+(r^+)\frac{\partial T^+}{\partial x^+} = \frac{1}{(r^+)^m}\frac{\partial}{\partial r^+}\left((r^+)^m\frac{\partial T^+}{\partial r^+}\right), \quad 0 < r^+ < 1, \quad x^+ > 0, \quad t^+ > 0;$$

$$T^+ = \sin \delta t^+ \quad \text{at} \quad x^+ = 0, \quad 0 \le r^+ \le 1, \quad t^+ > 0; \tag{2}$$

$$\frac{\partial T^+}{\partial t^+} = 0 \quad \text{at} \quad r^+ = 0, \quad x^+ > 0, \quad t^+ > 0;$$

$$\frac{1}{a^+}\frac{\partial T^+}{\partial t^+} + \frac{\partial T^+}{\partial r^+} + {\rm Bi}_{\rm ext}T^+ = 0 \quad \text{at} \quad r^+ = 1, \quad x^+ > 0, \quad t^+ > 0,$$

where the following dimensionless quantities have been utilized:

$$a^+ = \frac{(\rho C)_f R_1}{(\rho C)_s (R_2 - R_1)}, \quad \mathrm{Bi}_{ext} = \frac{h_{ext} R_1}{k_s}, \quad r^+ = \frac{r}{R_1}, \quad t^+ = \frac{t\alpha_f}{R_1^2},$$

$$T^+ = \frac{T - T_\infty}{T_0}, \quad u^+ = \frac{u}{\bar{u}}, \quad x^+ = \frac{x\alpha_f}{R_1^2 \bar{u}}, \quad \delta = \frac{\omega R_1^2}{\alpha_f},$$

and $u^+(r^+)$ is the dimensionless velocity profile, which is expressed in the form

$$u^+(r^+) = \begin{cases} \dfrac{2^m + 2}{2}(1 - (r^+)^2) & \text{for parabolic flow}, \\ 1 & \text{for slug flow}. \end{cases}$$

Here, we are interested in the periodic solution of the problem. We seek the solution as

$$T^+(x^+, r^+, t^+) = \tilde{T}^+(x^+, r^+) \exp(i\delta t^+), \tag{3}$$

where $i = \sqrt{-1}$. Substituting Eq. (3) into Eqs. (2), we obtain the following system:

$$i\delta \tilde{T}^+ + u^+(r^+) \frac{\partial \tilde{T}^+}{\partial x^+} = \frac{1}{(r^+)^m} \frac{\partial}{\partial r^+} \left((r^+)^m \frac{\partial \tilde{T}^+}{\partial r^+} \right), \quad 0 < r^+ < 1, \quad x^+ > 0;$$

$$\tilde{T}^+ = 1, \quad 0 \le r^+ \le 1, \quad x^+ = 0;$$

$$\frac{\partial \tilde{T}^+}{\partial r^+} = 0 \quad \text{at} \quad r^+ = 0, \quad x^+ > 0; \tag{4}$$

$$\frac{\partial \tilde{T}^+}{\partial r^+} + (\mathrm{Bi}_{ext} + ib^+) \tilde{T}^+ = 0 \quad \text{at} \quad r^+ = 0, \quad x^+ > 0,$$

where $b^+ = \delta / a^+$.

We define the Laplace transform of the complex temperature as

$$\bar{\tilde{T}}^+(r^+, s) = \int_0^\infty \exp(-sx^+) \tilde{T}^+(r^+, x^+) \, dx^+. \tag{5}$$

After the Laplace transformation with respect to the variable x^+, Eqs. (4) become

$$\frac{1}{(r^+)^m} \frac{\partial}{\partial r^+} \left((r^+)^m \frac{\partial \bar{\tilde{T}}^+}{\partial r^+} \right) = (i\delta + su^+(r^+)) \bar{\tilde{T}}^+ - u^+(r^+), \quad 0 < r^+ < 1; \tag{6}$$

$$\frac{\partial \bar{\tilde{T}}^+}{\partial r^+} = 0 \quad \text{at} \quad r^+ = 0, \quad x^+ > 0; \tag{6a}$$

$$\frac{\partial \bar{\tilde{T}}^+}{\partial r^+} = (\mathrm{Bi}_{ext} + ib^+) \bar{\tilde{T}}^+ \quad \text{at} \quad r^+ = 1, \quad x^+ > 0. \tag{6b}$$

The corresponding variational form of problem (6) that contains the boundary conditions is

$$I = \int_0^1 \left(\left(\frac{\partial \bar{\bar{T}}^+}{\partial r^+} \right)^2 + [su^+ (r^+) + i\delta] (\bar{\bar{T}}^+)^2 - 2u^+ \bar{\bar{T}}^+ \right) (r^+)^m dr^+ + (\mathrm{Bi}_{\mathrm{ext}} + ib^+) (\bar{\bar{T}}^+)^2 \big|_{r^+=1} = 0 \,. \tag{7}$$

On the other hand, the problem can be readily solved by the Ritz method. The first step of this method of analysis is the selection of a trial solution that must satisfy the boundary conditions. We approximate this solution by

$$\bar{\bar{T}}^+ (r^+, s) = \sum_{n=1}^{N} C_n (s) \cos (\sigma_n r^+) \,, \tag{7a}$$

where the function $\cos (\sigma_n r^+)$ satisfies the boundary conditions (6a) and (6b). The eigenvalues σ are the solutions of the transcendental equation

$$\sigma \tan \sigma = \mathrm{Bi}_{\mathrm{ext}} + ib^+ \,. \tag{7b}$$

Next we insert these trial solutions $\bar{\bar{T}}^+(r^+, s)$ into the variational expression (7) and require that the following equation be fulfilled:

$$\frac{\partial I (C_1,..., C_N)}{\partial C_i} = 0 \quad \text{for} \quad i = 1, ..., N \,. \tag{7c}$$

This procedure results in N algebraic equations for the determination of N unknown coefficients $C_i(s)$:

$$a_{11} C_1 (s) + ... + a_{1N} C_N (s) = b_1 \,,$$

$$.....$$

$$a_{N1} C_1 (s) + ... + a_{NN} C_N (s) = b_N \,. \tag{7d}$$

Equations (7d) can be expressed in a matrix form as $[A][C] = [B]$, where the symmetric square matrix $[A]$ can be written in the following way:

$$[A] = [A^*] + s\,[D] \,. \tag{7e}$$

The complex elements a_{ij}^* and d_{ij} of the matrices $[A^*]$ and $[D]$, respectively, and the elements b_i of the vector $[B]$ are presented in the Appendix for both duct geometries. We determine the dimensionless wall heat flux, centerline and wall temperatures, $\bar{\bar{q}}_{\mathrm{w}}(s)$, $\bar{\bar{T}}_{\mathrm{c}}(s)$, and $\bar{\bar{T}}_{\mathrm{w}}(s)$, from the following definitions:

$$\bar{\bar{q}}_{\mathrm{w}}^+ (s) = \left. \frac{\partial \bar{\bar{T}}^+}{\partial r^+} \right|_{r^+=1} = \sum_{n=1}^{N} C_n (s)\, \sigma_n \sin \sigma_n = \sum_{n=1}^{N} \frac{F_n}{s + \mu_n} \,,$$

$$\bar{\bar{T}}_{\mathrm{c}}^+ (s) = \sum_{n=1}^{N} C_n (s) = \sum_{1}^{N} \frac{A_n}{s + \mu_n} \,, \tag{8}$$

$$\bar{\bar{T}}_{\mathrm{w}}^+ (s) = \sum_{n=1}^{N} C_n (s) \cos\ \sigma_n = \sum_{n=1}^{N} \frac{W_n}{s + \mu_n} \,.$$

We also evaluate the dimensionless bulk temperature expressed as

$$\bar{\bar{T}}_{\mathrm{b}}^{+}(s) = (m+1)\int_0^1 (r^+)^m u^+(r^+)\,\bar{\bar{T}}^+(r^+, s)\,dr^+ =$$

$$= \begin{cases} 3\sum_1^N C_n(s)\left[\dfrac{\sin\sigma_n}{\sigma_n^3} - \dfrac{\cos\sigma_n}{\sigma_n^2}\right] & \text{for parallel-plate channel,} \\ 4\sum_1^N C_n(s)\left[6\left(\dfrac{\sin\sigma_n}{\sigma_n^3} + \dfrac{\cos\sigma_n - 1}{\sigma_n^4}\right) - \dfrac{2\cos\sigma_n + 1}{\sigma_n^2}\right] & \text{for circular duct,} \end{cases}$$

or

$$\bar{\bar{T}}_{\mathrm{b}}^{+}(s) = \sum_{n=1}^{N} \frac{Q_n}{s+\mu_n}. \tag{8a}$$

Here μ_n are the complex roots of the characteristic equation $\det[A] = 0$, and Q_n, F_n, W_n, and A_n are the complex quantities. The inverse transform of Eqs. (8) and (8a) may be written as

$$\begin{gathered} \tilde{q}_{\mathrm{w}}(x^+) = \sum_{n=1}^{N} F_n \exp(-\mu_n x^+), \quad \tilde{T}_{\mathrm{c}}^{+}(x^+) = \sum_{n=1}^{N} A_n \exp(-\mu_n x^+), \\ \tilde{T}_{\mathrm{w}}^{+}(x^+) = \sum_{n=1}^{N} W_n \exp(-\mu_n x^+), \quad \tilde{T}_{\mathrm{b}}^{+}(x^+) = \sum_{n=1}^{N} Q_n \exp(-\mu_n x^+). \end{gathered} \tag{9}$$

We solve Eqs. (9) by using five-term trial solutions and compute explicitly the quantities Q_n, F_n, W_n, A_n, and μ_n. This yields the accurate values of temperatures and wall heat flux. It is convenient to write

$$T_{\mathrm{c,w,b}}^{+}(x^+, t^+) = A_{\mathrm{c,w,b}}(x^+)\sin[\delta t^+ - \phi_{\mathrm{c,w,b}}(x^+)],$$

where

$$A_{\mathrm{c,w,b}}(x^+) = \left|\tilde{T}_{\mathrm{c,w,b}}^{+}(x^+)\right|, \quad \phi_{\mathrm{c,w,b}}(x^+) = -\arg\tilde{T}_{\mathrm{c,w,b}}^{+}(x^+),$$

and

$$q_{\mathrm{w}}(x^+, t^+) = A_{\mathrm{f}}(x^+)\sin[\delta t^+ - \phi_{\mathrm{f}}(x^+)],$$

where

$$A_{\mathrm{f}}(x^+) = \left|\tilde{q}_{\mathrm{w}}(x^+)\right|, \quad \phi_{\mathrm{f}}(x^+) = -\arg\tilde{q}_{\mathrm{w}}(x^+).$$

We determine the Nusselt number Nu as

$$\mathrm{Nu} = 2^{2-m} \frac{\left.\dfrac{\partial T^+(r^+, x^+, t^+)}{\partial r^+}\right|_{r^+=1}}{T^+(1, x^+, t^+) - T_\mathrm{b}^+(x^+, t^+)} . \tag{10}$$

Quasi-Steady Model. For comparison purposes, the same problem will also be solved with the aid of the quasi-steady model that uses the heat transfer coefficient at the interface. The mathematical formulation of this transient conjugated problem is given as

$$(\rho C)_\mathrm{f} \frac{R_1}{m+1} \left(\frac{\partial T_\mathrm{b}}{\partial t} + \overline{u} \frac{\partial T_\mathrm{b}}{\partial x} \right) = h_\mathrm{int} (T_\mathrm{w} - T_\mathrm{b}) , \quad x > 0 , \quad t > 0 ;$$

$$T_\mathrm{b} = T_\infty + T_0 \sin \omega t \qquad \text{at} \quad x = 0 , \quad t > 0 ; \tag{11}$$

$$(\rho C)_\mathrm{s} (R_2 - R_1) \frac{\partial T_\mathrm{w}}{\partial t} + h_\mathrm{ext} (T_\mathrm{w} - T_\infty) = h_\mathrm{int} (T_\mathrm{b} - T_\mathrm{w}) , \quad x > 0 .$$

Introducing the dimensionless parameters and complex temperatures, we obtain

$$i\delta \, \tilde{T}_\mathrm{b}^+ + \frac{\partial \tilde{T}_\mathrm{b}^+}{\partial x^+} = \frac{\mathrm{Nu}}{2^{2-2m}} (\tilde{T}_\mathrm{w}^+ - \tilde{T}_\mathrm{b}^+) , \quad x^+ > 0 ;$$

$$\tilde{T}_\mathrm{b}^+ (0) = 1 \qquad \text{at} \quad x^+ = 0 ; \tag{12}$$

$$\tilde{T}_\mathrm{w}^+ (ib^+ + \mathrm{Bi}_\mathrm{ext}) = \mathrm{Bi}_\mathrm{int} (\tilde{T}_\mathrm{b}^+ - \tilde{T}_\mathrm{w}^+) , \qquad x^+ > 0 ,$$

where the Nusselt and Biot numbers are given by

$$\mathrm{Nu} = 2^{2-m} \frac{h_\mathrm{int} R_1}{k_\mathrm{f}} , \qquad \mathrm{Bi}_\mathrm{int} \frac{\mathrm{Nu}}{2^{2-m}} . \tag{13}$$

The bulk temperature distribution is obtained as

$$\tilde{T}_\mathrm{b}^+ (x^+) = \exp (-\mu x^+) , \tag{14}$$

where

$$\mu = i\delta + \frac{\mathrm{Nu}}{2^{2-2m}} \frac{\mathrm{Bi}_\mathrm{ext} + ib^+}{\mathrm{Bi}_\mathrm{ext} + ib^+ + \mathrm{Bi}_\mathrm{int}} .$$

With μ being represented in the form $\mu = \eta + i\xi$, the bulk temperature is written as

$$\tilde{T}_\mathrm{b}^+ (x^+) = \exp (-\eta x^+) \exp (-i\xi x^+) . \tag{14a}$$

The bulk temperature amplitude and phase lag are given respectively by

$$\left| \tilde{T}_\mathrm{b}^+ (x^+) \right| = \exp (-\eta x^+) , \quad \phi_\mathrm{b} = -\arg \tilde{T}_\mathrm{b} = \xi x^+ . \tag{14b}$$

TABLE 1. The First Five Eigenvalues and Eigenfunctions Q_n for a Parallel-Plate Channel at $Bi_{ext} = 0$, $\delta = 0.1$, and Different Values of a^+

a^+	n	σ_n	μ_n	Q_n
$5\cdot10^{-5}$	1	0.15708E+1 + 0.79329E–3i	0.18853E+1 + 0.77654E–1i	0.98552E+0 – 0.25882E–3i
	2	0.47124E+1 + 0.22619E–2i	0.22425E+2 + 0.11362E+0i	0.12166E–1 + 0.11193E–3i
	3	0.78540E+1 + 0.41152E–2i	0.62304E+2 + 0.12944E+0i	0.15764E–2 + 0.48429E–4i
	4	0.10996E+2 + 0.56872E–2i	0.12454E+3 + 0.16183E+0i	0.41024E–3 + 0.25099E–4i
	5	0.14137E+2 + 0.66901E–2i	0.20809E+3 + 0.18957E+0i	0.15011E–3 + 0.14015E–4i
$8.5\cdot10^{-3}$	1	0.15592E+1 + 0.13329E+0i	0.18515E+1 + 0.34692E+0i	0.99917E+0 – 0.42268E–1i
	2	0.46701E+1 + 0.41943E+0i	0.22000E+2 + 0.15806E+1i	0.15459E–1 + 0.23974E–1i
	3	0.77383E+1 + 0.78019E+0i	0.61206E+2 + 0.50245E+1i	0.14385E–2 + 0.13759E–1i
	4	0.10560E+2 + 0.12734E+1i	0.12211E+3 + 0.88031E+1i	–0.71051E–2 + 0.10564E–1i
	5	0.12957E+2 + 0.13175E+1i	0.20367E+3 + 0.13291E+2i	–0.73814E–2 – 0.20592E–2i
0.1	1	0.80042E+0 + 0.57003E+0i	0.42142E+0 + 0.90514E+0i	0.10365E+1 + 0.54600E–1i
	2	0.31765E+1 + 0.32186E+0i	0.14107E+2 + 0.33612E+1i	–0.35812E–1 – 0.49497E–1i
	3	0.62874E+1 + 0.16049E+0i	0.46427E+2 + 0.34572E+1i	–0.60365E–3 – 0.38756E–2i
	4	0.94260E+1 + 0.10628E+0i	0.10143E+3 + 0.38954E+1i	–0.52089E–4 – 0.76592E–3i
	5	0.12567E+2 + 0.80036E–1i	0.17780E+3 + 0.42774E+1i	–0.92123E–5 – 0.24166E–3i

TABLE 2. The First Five Eigenfunctions for a Parallel-Plate Channel at $Bi_{ext} = 0$, $\delta = 0.1$, and Different Values of a^+

a^+	n	F_n	W_n	A_n
$5\cdot10^{-5}$	1	0.20000E+1 + 0.10227E–2i	–0.33897E–4 – 0.10100E–2i	0.12449E+1 + 0.52032E–3ii
	2	0.19999E+1 + 0.92281E–3i	–0.83231E–6 – 0.95991E–3i	–0.32999E+0 – 0.13746E–3i
	3	0.19994E+1 + 0.99106E–3i	0.21908E–5 – 0.10477E–2i	0.25458E+0 – 0.72161E–5i
	4	0.19988E+1 + 0.14373E–2i	0.95484E–6 – 0.10339E–2i	–0.18179E+0 – 0.36684E–4i
	5	0.19981E+1 + 0.14053E–2i	–0.16745E–5 – 0.94554E–3i	0.14133E+0 + 0.32530E–4i
$8.5\cdot10^{-3}$	1	0.20192E+1 + 0.18080E+0i	0.15395E–1 – 0.17161E+0i	0.12472E+1 + 0.94392E–2i
	2	0.23283E+1 + 0.31257E+0i	0.26569E–1 – 0.19795E+0i	–0.33414E+0 – 0.26800E–1i
	3	0.32062E+1 + 0.96563E+0i	0.82080E–1 – 0.27257E+0i	0.32518E+0 + 0.38002E–1i
	4	0.34191E+1 + 0.46362E+1i	0.39408E+0 – 0.29067E+0i	–0.26102E+0 – 0.12197E+0i
	5	–0.26679E+1 + 0.44148E+1i	0.37523E+0 + 0.22672E+0i	0.14108E+0 + 0.17294E+0i
0.1	1	0.33162E+0 + 0.92703E+0i	0.92708E+0 – 0.33164E+0i	0.10559E+1 + 0.13932E+0i
	2	–0.19955E+0 + 0.67601E–1i	0.67631E–1 + 0.19960E+0i	–0.58325E–1 – 0.15828E+0i
	3	–0.51671E–1 + 0.40559E–2i	0.40426E–2 + 0.51611E–1i	0.39571E–2 + 0.50956E–1i
	4	–0.22688E–1 + 0.77390E–3i	0.77593E–3 + 0.22730E–1i	–0.76869E–3 – 0.22603E–1i
	5	–0.12777E–1 + 0.24255E–3i	0.24202E–3 + 0.12730E–1i	0.24073E–3 + 0.12689E–1i

The temperature distribution in the solid is expressed as

$$\tilde{T}_w^+(x^+) = \frac{Bi_{int}}{Bi_{ext} + ib + Bi_{int}} \tilde{T}_b^+(x^+) .$$

Results and Discussion. Based on the variational analysis, we present the first five eigenvalues μ_n and σ_n and eigenfunctions Q_n, F_n, W_n, and A_n for a fully developed laminar flow inside a parallel-plate channel at different values of a^+ and $Bi_{ext} = 0$ in Tables 1 and 2. Tables 3 and 4 give the same coefficients for a circular duct. These values can be used in Eqs. (8) to calculate the wall heat flux and temperature distribution. For the purpose of comparison with the literature data, Tables 5 and 6 present the eigenvalues μ_n and coefficients A_n calculated by the variational model (VM) and those given by Li and Kakaç [13] using the generalized integral transform technique. As can be seen, the results obtained by these two approaches are in good agreement, which confirms the validity of the variational model.

In Fig. 2 we present the bulk temperature amplitudes and phase lags along the duct for a parallel-plate channel and a circular duct, respectively. The thermal capacitance ratio is fixed: $a^+ = 8.5\cdot10^{-3}$. This particular value corresponding to the practical case (the fluid is a gas and the wall is Styrofoam) is considered in [13]. It can be seen that the difference between the values of the phase lag obtained with the aid of the quasi-steady approach (QSA) and variational model (VM) is more significant for larger values of the dimensionless axial distance x^+. From these figures

TABLE 3. The First Five Eigenvalues and Eigenfunctions Q_n for a Circular Tube at $Bi_{ext} = 0$, $\delta = 0.1$, and Different Values of a^+

a^+	n	σ_n	μ_n	Q_n
	1	0.15708E+1 + 0.79329E–3i	0.36623E+1 + 0.65523E–1i	0.80085E+0 – 0.42493E–3i
	2	0.47124E+1 + 0.22619E–2i	0.22311E+2 + 0.83642E–1i	0.19445E+0 + 0.43881E–4i
$5\cdot10^{-5}$	3	0.78540E+1 + 0.41152E–2i	0.56967E+2 + 0.10538E+0i	–0.55018E–2 + 0.13032E–3i
	4	0.10996E+2 + 0.56872E–2i	0.10761E+3 + 0.13077E+0i	0.95969E–2 + 0.56909E–4i
	5	0.14137E+2 + 0.66901E–2i	0.17429E+3 + 0.14679E+0i	–0.17124E–2 + 0.38050E–4i
	1	0.15592E+1 + 0.13329E+0i	0.35643E+1 + 0.52628E+0i	0.81595E+0 – 0.70266E–1i
	2	0.46701E+1 + 0.41943E+0i	0.22018E+2 + 0.21268E+1i	0.21921E+0 + 0.16813E–1i
$8.5\cdot10^{-3}$	3	0.77383E+1 + 0.78019E+0i	0.56098E+2 + 0.45341E+1i	–0.54457E–2 + 0.35671E–1i
	4	0.10560E+2 + 0.12734E+1i	0.10577E+3 + 0.76177E+1i	–0.15489E–2 + 0.32484E–1i
	5	0.12957E+2 + 0.13175E+1i	0.17092E+3 + 0.11241E+2i	–0.23961E–1 – 0.60111E–2i
	1	0.80042E+0 + 0.57003E+0i	0.83570E+0 + 0.17625E+1i	0.10207E+1 – 0.11342E–1i
	2	0.31765E+1 + 0.32186E+0i	0.13267E+2 + 0.26901E+1i	–0.17751E–1 + 0.29038E–1i
0.1	3	0.62874E+1 + 0.16049E+0i	0.42264E+2 + 0.30307E+1i	–0.27904E–2 – 0.15356E–1i
	4	0.94260E+1 + 0.10628E+0i	0.87365E+2 + 0.32726E+1i	–0.11639E–3 – 0.88499E–3i
	5	0.12567E+2 + 0.80036E–1i	0.14853E+3 + 0.35518E+1i	–0.42716E–4 – 0.96539E–3i

TABLE 4. The First Five Eigenfunction for a Circular Tube at $Bi_{ext} = 0$, $\delta = 0.1$, and Different Values of a^+

a^+	n	F_n	W_n	A_n
	1	0.19999E+1 + 0.10172E–2i	–0.33898E–4 – 0.10100E–2i	0.12732E+1 + 0.46332E–5i
	2	0.20001E+1 + 0.93915E–3i	–0.82460E–6 – 0.96001E–3i	–0.42443E+0 + 0.44244E–5i
$5\cdot10^{-5}$	3	0.19991E+1 + 0.96349E–3i	0.21761E–5 – 0.10475E–2i	0.25454E+0 – 0.10704E–4i
	4	0.19993E+1 + 0.14750E–2i	0.97440E–6 – 0.10341E–2i	–0.18183E+0 – 0.40093E–4i
	5	0.19975E+1 + 0.13558E–2i	–0.16972E–5 – 0.94527E–3i	0.14129E+0 + 0.29047E–4i
	1	0.20192E+1 + 0.18080E+0i	0.15395E–1 – 0.17161E+0i	0.12841E+1 + 0.32045E–2i
	2	0.23283E+1 + 0.31258E+0i	0.26569E–1 – 0.19795E+0i	–0.46013E+0 – 0.12477E–1i
$8.5\cdot10^{-3}$	3	0.32062E+1 + 0.96562E+0i	0.82079E–1 – 0.27257E+0i	0.32518E+0 + 0.38000E–1i
	4	0.34192E+1 + 0.46362E+1i	0.39409E+0 – 0.29067E+0i	–0.26102E+0 – 0.12198E+0i
	5	–0.26679E+1 + 0.44148E+1i	0.37523E+0 + 0.22672E+0i	0.14108E+0 + 0.17294E+0i
	1	0.33160E+0 + 0.92703E+0i	0.92708E+0 – 0.33164E+0i	0.10589E+1 + 0.15428E+0i
	2	–0.19955E+0 + 0.67603E–1i	0.67633E–1 + 0.19960E+0i	–0.62243E–1 – 0.19049E+0i
0.1	3	–0.51673E–1 + 0.40527E–2i	0.40393E–2 + 0.51613E–1i	0.39539E–2 + 0.50958E–1i
	4	–0.22688E–1 + 0.77552E–3i	0.77756E–3 + 0.22731E–1i	–0.77031E–3 – 0.22603E–1i
	5	–0.12778E–1 + 0.23952E–3i	0.23899E–3 + 0.12731E–1i	0.23772E–3 + 0.12690E–1i

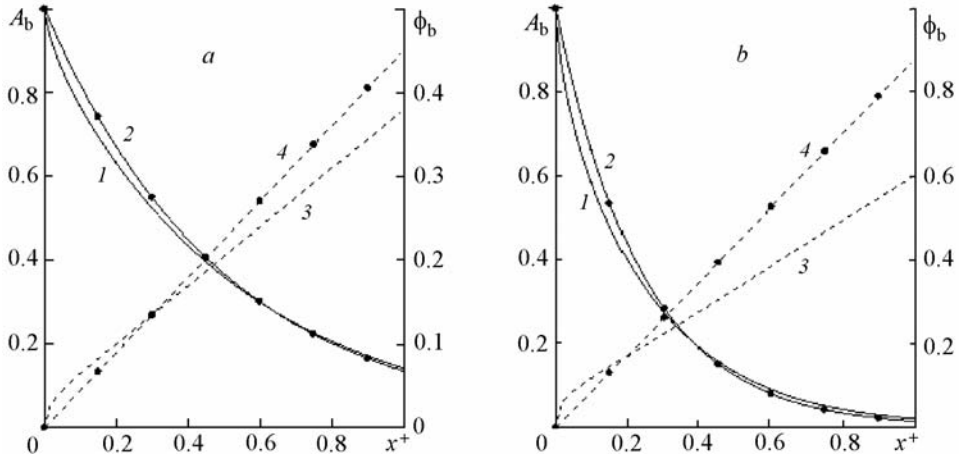

Fig. 2. Amplitude (1 and 2) and phase lag (3 and 4) of the bulk temperature for parallel-plate (a) and circular (b) ducts as functions of the axial distance at $a^+ = 8.5\cdot10^{-3}$, $\delta = 0.1$, and $Bi_{ext} = 0$. The curves 1, 3 correspond to the VM and 2, 4 to the QSA. ϕ_b, rad.

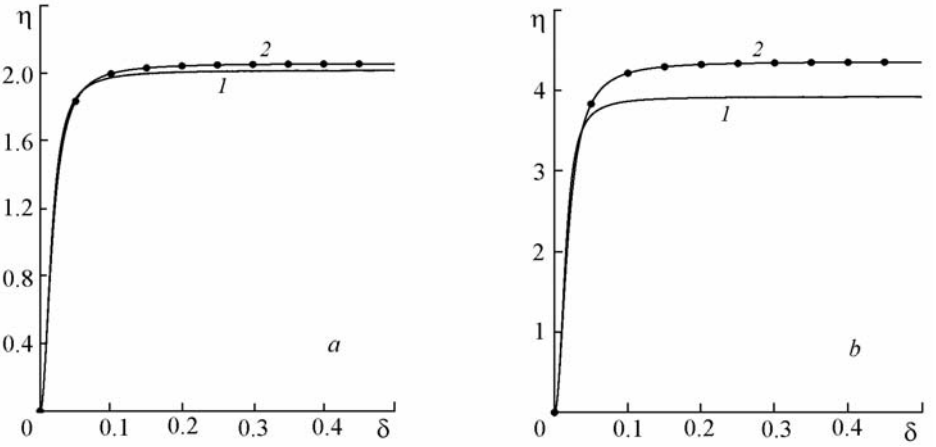

Fig. 3. Damping coefficient as a function of δ for parallel-plate (a) and circular (b) ducts in the VM (1) and QSA (2) cases.

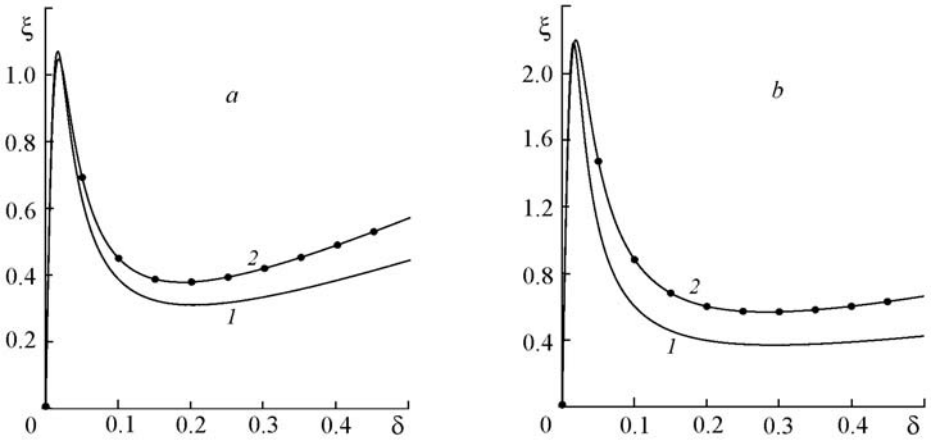

Fig. 4. Phase lag coefficient as a function of δ for parallel-plate (a) and circular (b) ducts in the VM (1) and QSA (2) cases. ξ, rad.

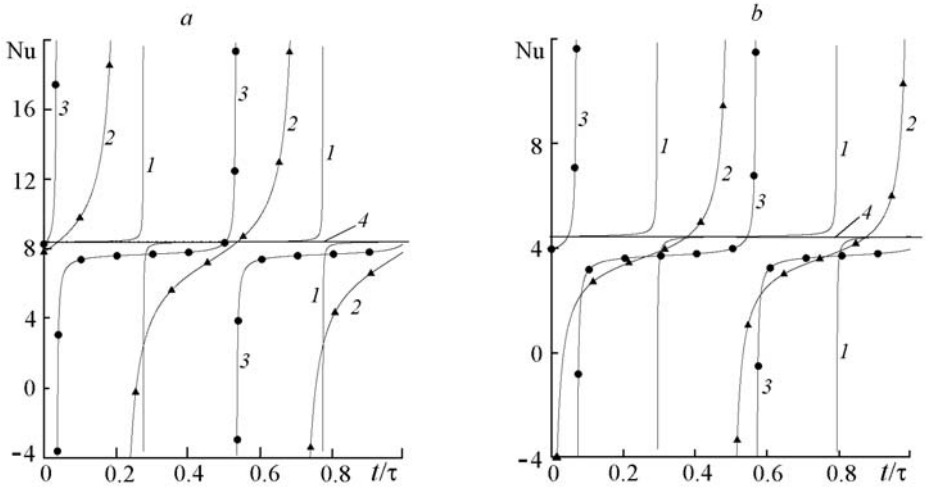

Fig. 5. Time dependence of the Nusselt number at $x^+ = 1$ for parallel-plate (a) and circular (b) ducts with different values of δ: 1) $\delta = 10^{-3}$; 2) 0.1; 3) 10. The line 4 corresponds to a steady-state value.

TABLE 5. The First Two Eigenvalues and Coefficients for a Parallel-Plate Channel from the Present Study and [13] at $Bi_{ext} = 0$, $\delta = 0.1$, and Different Values of a^+

a^+	A_n		μ_n	
	Present study	[13]	Present study	[13]
$5\cdot10^{-5}$	0.12449E+1 + 0.52032E–3i	0.12072E+1 + 0.82011E–3i	0.18853E+1 + 0.77654E–1i	0.20117E+1 + 0.72862E–1i
	–0.32999E+0 – 0.13746E–3i	–0.31090E+0 – 0.95008E–3i	0.22425E+2 + 0.11362E+0i	0.22407E+2 + 0.10293E+0i
$8.5\cdot10^{-3}$	0.12472E+1 + 0.94392E–2i	0.12093E+1 + 0.14771E–1i	0.18515E+1 + 0.34692E+0i	0.19728E+1 + 0.37485E+0i
	–0.33414E+0 – 0.26800E–1i	–0.31598E+0 – 0.27488E–1i	0.22000E+2 + 0.15806E+1i	0.22009E+2 + 0.24615E+1i
0.1	0.10559E+1 + 0.13932E+0i	0.10648E+1 + 0.11674E+0i	0.42142E+0 + 0.90514E+0i	0.40422E+0 + 0.92886E+0i
	–0.58325E–1 – 0.15828E+0i	–0.72035E–1 – 0.15280E+0i	0.14107E+2 + 0.33612E+1i	0.12772E+2 + 0.28317E+1i

TABLE 6. The First Two Eigenvalues and Coefficients for a Parallel-Plate Channel from the Present Study and [13] at $a^+ = 8.5\cdot10^{-3}$, $\delta = = 0.1$, and Different Values of Bi_{ext}

Bi_{ext}	A_n		μ_n	
	Present study	[13]	Present study	[13]
0.1	0.12471E+1 + 0.94842E–2i	0.12083E+1 + 0.14892E3–1i	0.18493E+1 + 0.34632E+0i	0.19703E+1 + 0.37647E+0i
	–0.33388E+0 – 0.26873E–1i	–0.31556E+0 – 0.27771E–1i	0.21991E+2 + 0.15739E+1i	0.21986E+2 + 0.24723E+1i
1.0	0.12464E+1 + 0.98363E–2i	0.12073E+1 + 0.16102E–1i	0.18300E+1 + 0.33931E+0i	0.19432E+1 + 0.38806E+0i
	–0.33149E+0 – 0.27282E–1i	–0.31352E+0 – 0.30440E–1i	0.21919E+2 + 0.15117E+1i	0.21762E+2 + 0.25467E+1i
10	0.12564E+1 + 0.58462E–2i	0.11935E+1 + 0.13486E–1i	0.17486E+1 + 0.21693E+0i	0.17378E+1 + 0.27210E+0i
	–0.37173E+0 – 0.15623E–1i	–0.28560E+0 – 0.25321E–1i	0.20393E+2 + 0.11081E+1i	0.20283E+2 + 0.15247E+1i

it is clear that this deviation for a circular duct is more pronounced than for a parallel-plate channel. We note that for the bulk temperature amplitude the two approaches are equivalent except for a short distance from the inlet ($x^+ < 0.1$). As follows from Eq. (14b), the amplitude of the bulk temperature is damped exponentially with the axial distance and the phase lag increases linearly along the duct.

Figure 3 shows that the values of the damping coefficient η obtained by the QSA agree very well with those extracted from the VM for lower values of δ ($\delta < 0.1$). For higher values of δ ($\delta > 0.1$), the relative deviation is stable and equal to 2.5% and 12% respectively for a parallel-plate channel and circular duct, and the parameter η becomes insensitive to the inlet frequency. In Fig. 4 the phase lag coefficient ξ is presented as a function of the inlet temperature frequency in both ducts. We note the same behavior as for the damping coefficient η, but the discrepancy between the two solutions is more appreciable: it ranges up to 33% for a circular tube and 23% for a parallel-plate channel at $\delta = 0.3$.

Finally, in Fig. 5 we present the Nusselt number as a function of time at $x^+ = 1$ in the parallel-plate and circular ducts for various values of the inlet frequency (here $\tau = 2\pi/\omega$ is the period). When the bulk and wall temperatures are close and the heat flow is not zero, the Nusselt number tends to infinity. When $T_b < T\big|_{r^+=1}$, the heat flux from the wall to the fluid and the Nusselt number tend to $+\infty$. When T_b becomes larger than $T\big|_{r^+=1}$, the heat flux changes its direction, and the Nuselt number tends to $-\infty$. On the other hand, we remark that for a lower inlet frequency ($\delta = 0.001$) the horizontal portion of the Nusselt number curve is closely related to the known steady-state Nusselt number (line 4) that corresponds to Nu = 8.24 and 4.36 respectively for the parallel-plate channel and circular duct. For a higher inlet frequency ($\delta = 0.1$–10), the instantaneous Nusselt number will become highly time-dependent and the QSA is inadequate.

APPENDIX

The complex elements of the matrices $[A^*]$ and $[D]$ for a parallel-plate channel look like

$$a_{ii}^* = \sigma_i^2\left(1 - \frac{\sin 2\sigma_i}{2\sigma_i}\right) + i\delta\left(1 + \frac{\sin 2\sigma_i}{2\sigma_i}\right) + 2\sigma_i \sin\sigma_i \cos\sigma_i ,$$

$$a^*_{ij(i\neq j)} = \sigma_i\sigma_j\left(\frac{\sin(\sigma_i-\sigma_j)}{\sigma_i-\sigma_j}-\frac{\sin(\sigma_i+\sigma_j)}{\sigma_i+\sigma_j}\right)+i\delta\left(\frac{\sin(\sigma_i-\sigma_j)}{\sigma_i-\sigma_j}+\frac{\sin(\sigma_i+\sigma_j)}{\sigma_i+\sigma_j}\right)+2\sigma_i\sin\sigma_i\cos\sigma_j,$$

$$d_{ii} = 1+\frac{3}{2}\left(\frac{\sin 2\sigma_i}{4\sigma_i^3}-\frac{\cos 2\sigma_i}{2\sigma_i^2}\right),$$

$$d_{ij(i\neq j)} = 3\left(\frac{\sin(\sigma_i-\sigma_j)}{(\sigma_i-\sigma_j)^3}+\frac{\sin(\sigma_i+\sigma_j)}{(\sigma_i+\sigma_j)^3}-\frac{\cos(\sigma_i-\sigma_j)}{(\sigma_i-\sigma_j)^2}-\frac{\cos(\sigma_i+\sigma_j)}{(\sigma_i+\sigma_j)^2}\right).$$

The vector [B] is defined as

$$b_i = 6\left(\frac{\sin\sigma_i}{\sigma_i^3}-\frac{\cos\sigma_i}{\sigma_i^2}\right).$$

The complex elements of the matrices [A^*] and [D] for a circular duct take the form

$$a^*_{ii} = \frac{\sigma_i^2}{2}\left(1-\frac{\sin 2\sigma_i}{\sigma_i}-\frac{\cos 2\sigma_i-1}{4\sigma_i^2}\right)+\frac{i\delta}{2}\left(1+\frac{\sin 2\sigma_i}{\sigma_i}+\frac{\cos 2\sigma_i-1}{2\sigma_i^2}\right)+2\sigma_i\sin\sigma_i\cos\sigma_i,$$

$$a^*_{ij(i\neq j)} = \sigma_i\sigma_j\left(\frac{\sin(\sigma_i-\sigma_j)}{\sigma_i-\sigma_j}-\frac{\sin(\sigma_i+\sigma_j)}{\sigma_i+\sigma_j}+\frac{\cos(\sigma_i-\sigma_j)-1}{(\sigma_i-\sigma_j)^2}-\frac{\cos(\sigma_i+\sigma_j)-1}{(\sigma_i+\sigma_j)^2}\right)$$

$$+i\delta\left(\frac{\sin(\sigma_i-\sigma_j)}{\sigma_i-\sigma_j}+\frac{\sin(\sigma_i+\sigma_j)}{\sigma_i+\sigma_j}+\frac{\cos(\sigma_i-\sigma_j)-1}{(\sigma_i-\sigma_j)^2}+\frac{\cos(\sigma_i+\sigma_j)-1}{(\sigma_i+\sigma_j)^2}\right)+2\sigma_i\sin\sigma_i\cos\sigma_j,$$

$$d_{ii} = \frac{1}{2\sigma_i^2}\left(1+\frac{3\sin 2\sigma_i}{\sigma_i}+\frac{3(\cos 2\sigma_i-1)}{2\sigma_i^2}-(2\cos 2\sigma_i+1)\right),$$

$$d_{ij(i\neq j)} = \frac{2}{(\sigma_i-\sigma_j)^2}\left(\frac{6\sin(\sigma_i-\sigma_j)}{\sigma_i-\sigma_j}+\frac{6(\cos(\sigma_i-\sigma_j)-1)}{(\sigma_i-\sigma_j)^2}-(2\cos(\sigma_i-\sigma_j)+1)\right)$$

$$+\frac{2}{(\sigma_i+\sigma_j)^2}\left(\frac{6\sin(\sigma_i+\sigma_j)}{\sigma_i+\sigma_j}+\frac{6(\cos(\sigma_i+\sigma_j)-1)}{(\sigma_i+\sigma_j)^2}-(2\cos(\sigma_i+\sigma_j)+1)\right).$$

The vector [B] is defined by

$$b_i = 4\left(\frac{6\sin\sigma_i}{\sigma_i^3}+\frac{6(\cos\sigma_i-1)}{\sigma_i^4}-\frac{2\cos\sigma_i+1}{\sigma_i^2}\right).$$

NOTATION

a^*_{ij} and d_{ij}, complex elements of the matrices [A^*] and [D], respectively; a^+, fluid-to-wall thermal capacitance ratio; $A(x^+)$, dimensionless temperature amplitude; B_i and C_i, elements of the vectors [B] and [C]; Bi, Biot number; h, convection heat transfer coefficient, $W\cdot m^{-2}\cdot K^{-1}$; k, termal conductivity, $W\cdot m^{-1}\cdot K^{-1}$; q_w, wall heat flux; r, radial or normal coordinate, m; R_1, radius of circular duct or half the spacing between parallel plates, m; R_2, outer radius, m; s, Laplace transform variable; T, fluid temperature, K; T_∞, ambient temperature, K; T_0, amplitude of inlet temperature, K;

t, time, sec; u, flow velocity, m·sec^{-1}; $\bar{u}$, mean velocity, m·sec^{-1}; x, axial coordinate, m; α, thermal diffusivity, m^2·sec^{-1}; δ, dimensionless inlet frequency; η, damping coefficient; μ_n, complex root of the characteristic equation; ξ, phase lag coefficient, rad; ρ, density, kg·m^{-3}; σ_n, eigenvalue; ϕ, phase lag, rad; ω, inlet frequency, Hz. Subscripts and superscripts: b, bulk; c, centerline; e, external; f, fluid; int, internal; s, solid; w, wall; +, dimensionless quantity; the overbar denotes the Laplace transform with respect to the x^+ variable.

REFERENCES

1. S. Kakaç and Y. Yener, Exact solution of transient forced convection energy equation for timewise variation of inlet temperature, *Int. J. Heat Mass Transfer*, **16**, 2205–2214 (1973).
2. S. Kakaç and Y. Yener, Frequency response analysis of transient turbulent forced convection for timewise variation of inlet temperature, in: S. Kakaç and D. B. Spalding (Eds), *Turbulent Forced Convection in Channels and Bundles*, Hemisphere Publishing Corporation, New York (1979), pp. 865–880.
3. R. M. Cotta and M. N. Ozisik, Laminar forced convection inside ducts with periodic variation of inlet temperature, *Int. J. Heat Mass Transfer*, **29**, 1445–1501 (1986).
4. W. S. Kim and M. N. Ozisik, Turbulent forced convection inside a parallel-plate channel with periodic variation of inlet temperature, *Trans. ASME, J. Heat Transfer*, **111**, 882–888 (1989).
5. M. Arik, C. A. C. Santos, and S. Kakaç, Turbulent forced convection with sinusoidal variation of inlet temperature between two parallel plates, *Int. Commun. Heat Mass Transfer*, **23**, 1121–1132 (1996).
6. M. Unsal, A solution for the complex eigenvalues and eigenfunctions of the periodic Graetz problem, *Int. Commun. Heat Mass Transfer*, **25**, No. 4, 585–592 (1998).
7. E. M. Sparrow and F. N. De Farias, Unsteady heat transfer in ducts with time varying inlet temperature and participating walls, *Int. J. Heat Mass Transfer*, **11**, 837–853 (1968).
8. R. M. Cotta, M. D. Mikhailov, and M. N. Ozisik, Transient conjugated forced convection in ducts with periodically varying inlet temperature, *Int. J. Heat Mass Transfer*, **30**, 2073–2082 (1987).
9. W. S. Kim and M. N. Ozisik, Conjugated laminar forced convection in ducts with periodic variation of inlet temperature, *Int. J. Heat Fluid Flow*, **11**, 311–320 (1990).
10. J. S. Travelho and F. N. Santos, Solution for transient conjugated forced convection in the thermal entrance region of a duct with periodically varying inlet temperature, *Trans. ASME, J. Heat Transfer*, **113**, 558–562 (1991).
11. J. S. Travelho and F. N. Santos, Unsteady conjugate heat transfer in a circular duct with convection from the ambient and periodically varying inlet temperature, *Trans. ASME, J. Heat Transfer*, **120**, 506–510 (1998).
12. S. Kakaç and W. Li, Unsteady turbulent forced convection in a parallel-plate channel with timewise variation of inlet temperature, *Int. J. Heat Mass Transfer*, **37**, 447–456 (1994).
13. W. Li and S. Kakaç, Unsteady thermal entrance heat transfer in laminar flow with a periodic variation of inlet temperature, *Int. J. Heat Mass Transfer*, **34**, 2581–2592 (1991).
14. B. Fourcher and K. Mansouri, An approximate analytical solution to the Graetz problem with periodic inlet temperature, *Int. J. Heat Fluid Flow*, **18**, 229–235 (1997).
15. K. Mansouri and B. Fourcher, The effects of inlet temperature frequency on the quasi-steady approach of periodic conjugated heat transfer problem, *Int. J. Eng. Sci.*, **42**, 825–839 (2004).
16. R. O. C. Guedes and R. M. Cotta, Periodic laminar forced convection within ducts including wall heat conduction effects, *Int. J. Eng. Sci.*, **29**, 535–547 (1991).
17. R. O. C. Guedes, M. N. Ozisik, and R. M. Cotta, Conjugated periodic turbulent forced convection in a parallel-plate channel, *Trans. ASME, J. Heat Transfer*, **116**, 40–46 (1994).
18. K. Mansouri and A. Hadiouche, On the solution of a periodic internal laminar flow, in: *Proc. CHT-08 Int. Symp. on Advances in Computational Heat Transfer*, Morocco, May 11–16, 2008, Begell House (2008).
19. G. D. Ngoma and F. Erchiqui, Heat transfer and slip effects on liquid flow in a micro-channel, *Int. J. Thermal Sci.*, **46**, 1076–1083 (2007).

20. W. Sun, S. Kakaç, and A. G. Yazicioglu, A numerical study of single phase convective heat transfer in micro-tubes for slip flow, *Int. J. Thermal Sci.*, **46**, 2581–2592 (2007).
21. J. Peixinho, C. Desaubry, and M. Lebouché, Heat transfer of non-Newtonian fluid (Carbopol aqueous solution) in transitional pipe flow, *Int. J. Heat Mass Transfer*, **51**, 195–209 (2008).
22. F. Tamisli, Laminar flow of a non-Newtonian fluid in channels with wall suction or injection, *Int. J. Eng. Sci.*, **44**, 650–661 (2006).
23. O. Jambal, T. Shigechi, G. Davaa, and S. Momki, Effects of viscous dissipation and fluid axial heat convection on heat transfer for non-Newtonian fluids in ducts with uniform wall temperature, *Int. Comm. Heat Mass Transfer*, **32**, 1165–1173 (2005).